sustainability

MDPI

Article

Linking Energy Management and Optical Calibration Quality for Sustainable Automotive Electronics Manufacturing: An IMES Case Study of Rain and Light Sensors

Oana Roxana Chivu [1,*], Demetrius Dubic (Petrescu) [1], Andrei Ştefan Iacob [1], Cătălina Enache [1], Marilena Gheorghe [1], Edward Petzek [2,*] and Anamaria Ioana Feier [3,*]

[1] Department of Quality Engineering and Industrial Technologies, Faculty of Industrial Engineering and Robotics, National University of Science and Technology Politehnica Bucharest, 313 Splaiul Independenței, 060042 Bucharest, Romania; andrei.iacob1808@upb.ro (A.Ş.I.); catalina.enache@upb.ro (C.E.)
[2] Department of Steel Structures and Structural Mechanics, SSF Romania, 1 Ioan Curea Street, 300224 Timișoara, Romania
[3] Department of Materials and Manufacturing Engineering, Faculty of Mechanical Engineering, Politehnica University of Timișoara, 1 Mihai Viteazu Boulevard, 300222 Timișoara, Romania
* Correspondence: oana.chivu@upb.ro (O.R.C.); epetzek@ssf.ro (E.P.); anamaria.feier@upt.ro (A.I.F.)

Abstract

Sustainable manufacturing requires managing energy efficiency and product quality jointly, yet automotive electronics plants typically handle them separately, despite sharing the same monitoring infrastructure. This case study examines a Volkswagen MQB-platform line producing headlight switching modules and windshield rain/light sensors (RLS), assessing the energy-saving potential of an Industrial Energy Management System (IMES) and RLS optical calibration as a source of avoidable retests and rejections. The energy assessment combined process analysis, published evidence and ISO 50001 requirements, without metering; the metrological assessment used calibration-bench data, automated test logs and end-of-line (EOL) records. Raising the correction factor from 0.02 to 0.03 increased the signal in all ten paired repetitions (+0.84% and +1.03%; paired t-test, $p < 0.001$) and reduced out-of-range Channel A readings from seven to one; linearity was not assessed. Test records without alerts accounted for 87.4–98.2%. All eight EOL units passed, yet positional deviations reached ±38.5 against a ±1.0 tolerance, warranting specification review. IMES adoption is projected, from the literature, to reduce energy consumption by 15–25% per unit. An energy-per-conforming-unit indicator links both: fewer false alerts, retests and rejections lower the energy, material and emission footprint of each sensor, supporting resource-efficient, low-carbon production (SDGs 9, 12 and 13).

Keywords: sustainable manufacturing; industrial energy management; energy efficiency; ISO 50001; energy per conforming unit; resource efficiency; zero-defect manufacturing; automotive electronics; rain and light sensor; optical calibration

Check for updates

Received: 21 September 2026
Revised: 21 October 2026
Accepted: 26 October 2026
Published: 30 October 2026

Copyright: © 2026 by the authors. Licensee MDPI, Basel, Switzerland. This article is an open access article distributed under the terms and conditions of the Creative Commons Attribution (CC BY) license.

1. Introduction

Energy consumption is a central lever for the sustainability of manufacturing, and integrating energy-efficiency performance into production management—rather than treating energy as a facility-level utility cost—has long been identified as a gap between industrial needs and the scientific literature [1]. Energy-related key performance indicators (KPIs) defined at machine, process and line level are the main instrument for closing that gap [2,3]. An Industrial Energy Management System (IMES) puts this idea into practice: it tracks

the energy- and equipment-related KPIs of an automated line, supports the definition of maintenance and energy-efficiency strategies, and helps to increase equipment availability and reduce operating costs [4–6]. By combining real-time data analytics with energy-consumption indicators, an IMES allows manufacturers to identify inefficiencies and to apply targeted adjustments to individual production stages [7].

Three developments shape current IMES practice. First, energy management is increasingly structured around ISO 50001 [8], which formalizes the energy review, energy performance indicators (EnPIs), energy baselines and continual improvement; firm-level evidence associates ISO 50001 adoption with a measurable reduction in manufacturing energy intensity [9], and projections of its global uptake indicate a substantial potential for energy and emission savings [10]. Second, Industrial Internet of Things (IIoT) retrofits and digital twins make it possible to monitor and optimize existing equipment in real time: an IIoT retrofit of a legacy machine exposed a compressed-air leak whose correction reduced its energy consumption by 56% [11], digital-twin methods allow real-time energy optimization of a production line under fault disturbances [12], and a systematic review of fifty digital-twin studies reported savings of up to 30%, together with persistent barriers of investment cost, cybersecurity and integration [13]. Third, a large share of manufacturing energy is consumed while equipment is idle; operational policies that switch non-bottleneck machines to low-power states during idle periods can reduce consumption substantially [14]. In electronics assembly, this applies in particular to reflow soldering ovens, for which energy performance measurement systems and stand-by strategies have been proposed [15,16].

Automotive electronics manufacturing is a demanding setting for such systems, because energy-intensive thermal processes coexist on the same line with high-precision optical and electrical testing. The windshield rain/light sensor (RLS) illustrates this coexistence. Its ambient-light channels supply the signal for automatic headlamp switching, a function governed by UN Regulation No. 48 on the installation of lighting and light-signaling devices [17], while its rain channel drives the automatic wiper function, whose responsiveness to rainfall intensity has been the subject of dedicated embedded-systems research [18]. Because both functions affect the driver's effective visibility, the sensor must be calibrated in a traceable and repeatable way at the end of the production line. The module and sensor examined here are produced for the Volkswagen Group's MQB platform, a modular architecture shared by many vehicle models; a systematic calibration deviation in a component of this kind is therefore multiplied across a correspondingly large production volume.

Energy monitoring and equipment reliability draw on the same data. Reliability, availability, maintainability and safety (RAMS) analysis, developed mainly for railway vehicles and infrastructure [19–23], derives inspection and maintenance intervals from measured failure and repair data rather than from fixed calendars. For automated production lines, the same logic has led to group-maintenance [24,25], availability-oriented [26] and condition-based maintenance models [27–29]. In Industry 4.0, these approaches have converged with data-driven predictive maintenance [30], although most studies based on artificial intelligence still use benchmark datasets rather than production records [31]. Energy data are themselves a diagnostic signal: anomalous consumption patterns have been used to detect faults in distributed manufacturing systems [32] and in industrial cyber-physical systems [33].

On the quality side, Pareto analysis combined with the eight-discipline (8D) problem-solving method [34] and the Six Sigma DMAIC (Define–Measure–Analyze–Improve–Control) cycle combined with failure mode and effects analysis (FMEA) [35] remain standard tools for prioritizing and eliminating defects in automotive manufacturing. Zero-defect manufacturing extends this perspective by treating defect prevention, detection, repair and

prediction as a route to reducing the waste associated with defective output [36]. This view connects product quality directly with resource efficiency: every false rejection, retest or rework operation consumes energy without adding conforming output.

These strands converge on the sustainability of manufacturing in three complementary ways. Environmentally, the electricity drawn by thermal processes and by idle equipment is a source of indirect greenhouse-gas emissions, so that verified reductions in energy intensity also reduce the emissions associated with each product, which is why ISO 50001 has been assessed as an instrument for climate change mitigation [9,10]. In terms of resources, every unit that is scrapped, reworked or retested because of a calibration or test problem carries with it the materials—printed circuit boards, electronic components, optical parts and housings—and the energy already embodied in it, so that first-pass yield is itself an indicator of resource efficiency [36]. Socially, the RLS is a safety-relevant component: accurate automatic headlamp and wiper switching supports driver visibility and therefore road safety [17,18]. Monitoring energy and calibration quality on the same line therefore addresses the objectives of responsible consumption and production (UN Sustainable Development Goal, SDG 12), climate action (SDG 13) and sustainable industry and innovation (SDG 9), and, through the safety function of the product, the road-safety target of SDG 3 (target 3.6).

Most of the studies cited above treat energy management and product quality separately. Energy studies typically address a single machine or utility system [11–13], whereas maintenance and quality studies typically address equipment strategy or defect categories without reference to energy [24–26,30,31]. Building on the authors' earlier work on smart manufacturing and occupational safety in the automotive sector [37,38] and on process-parameter monitoring in automotive component production [39], the present case study examines both dimensions on a single MQB-platform line for headlight switching modules and RLS, using production and test-bench records. The study has three aims: (i) to estimate, from a stage-level process analysis and published evidence, the energy-saving potential of IMES adoption at each manufacturing stage, and to specify how the IMES would be integrated with ISO 50001; (ii) to quantify, from bench measurements, the effect of changing the optical correction factor (CF) on the light-transmission readings of the calibration test benches; and (iii) to characterize, from automated test logs and EOL records, the alert patterns and calibration deviations that currently limit production tolerances. Aims (ii) and (iii) rest on measured data; aim (i) yields literature-based projections, which are identified as such throughout the paper. Taken together, the three aims treat energy efficiency and calibration quality as two levers of the same sustainability objective—lower energy, material and emission intensity per conforming unit—and the energy-per-conforming-unit indicator proposed in Section 2.2 is intended to make that objective measurable on the line. Section 2 describes the product, the manufacturing process, the energy-monitoring architecture and the test systems; Section 3 reports the measured results; Section 4 discusses them, together with the limitations of the study and the resulting future work; and Section 5 presents the conclusions.

2. Materials and Methods

2.1. Product and Sensor Description

The headlight switching module is the selector, mounted on the dashboard or on the turn-signal lever, through which the driver chooses the lighting function: OFF (all lights disconnected); AUTO (the ambient-light sensor decides when to switch the low beam or daytime running lights on or off, for example when entering a tunnel or driving at dusk); low beam; high beam; and dedicated fog-light and turn-signal positions (Figure 1). The selector sends commands to the vehicle's electronic control unit (ECU), which activates

the corresponding lamps on the basis of the selected position and of sensor data such as ambient light, steering angle and vehicle speed.

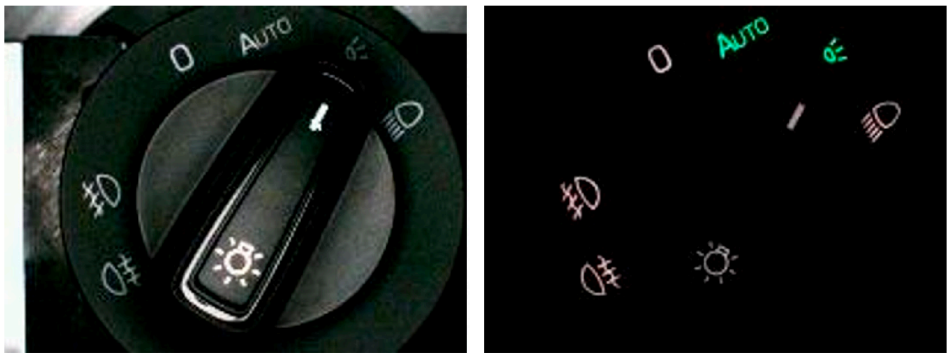


Figure 1. Headlight switching selector: daylight view of the physical control (**left**) and its illuminated symbols (**right**).

The RLS combines two optical measurement principles in a single housing mounted on the inner surface of the windshield, behind the rear-view mirror (Figure 2). Rain detection relies on total internal reflection [40]: infrared LEDs project light onto the outer glass–air interface at an angle larger than the critical angle of a dry windshield (about 42° for typical automotive glass), so that the light is reflected back onto a photodiode array. When water covers the outer surface, the critical angle rises to roughly 61°, part of the light is transmitted into the water film, and the drop in photodiode signal is used to infer the presence and intensity of rain. Ambient-light detection uses a separate pair of photodiodes—the forward channel (Channel A, ChA) and the global channel (Channel B, ChB)—fitted with spectral filters that approximate the spectral luminous efficiency function of the human eye [41], so that the measured signal correlates with perceived brightness rather than with raw irradiance. The sensor communicates with the vehicle through the Local Interconnect Network (LIN) protocol [42].

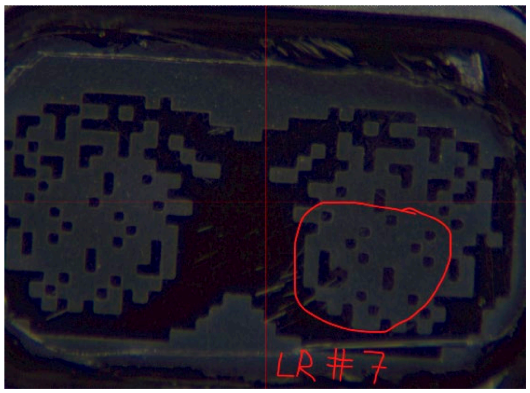


Figure 2. Windshield-mounted rain and light sensor; the circled area (LR #7) marks the location of a localized positional-calibration deviation of the type analyzed in Section 3.3. Windshield-mounted rain and light sensor; the area outlined in red and labeled LR #7 marks the location of a localized positional-calibration deviation of the type analyzed in Section 3.3.

2.2. Manufacturing Process, Energy-Monitoring Architecture and ISO 50001 Integration

The headlight switching module is produced in five main stages—printed circuit board (PCB) manufacturing, component assembly, soldering, functional testing and encapsulation—each instrumented for energy consumption, alarms and equipment efficiency under a common energy control and monitoring layer (Figure 3). The same

data-acquisition layer also serves the RLS calibration and EOL test benches described in Sections 2.3 and 2.4.

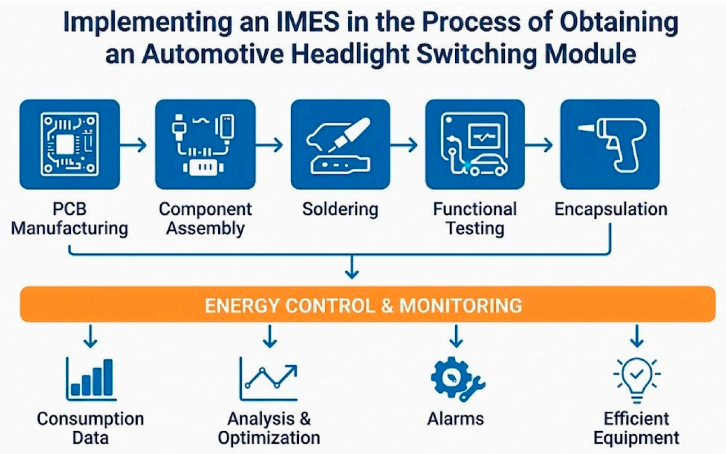


Figure 3. IMES-integrated production process for the automotive headlight switching module.

Three stages were analyzed in more detail because of their expected contribution to total energy demand:

- PCB production: low-consumption technologies (e.g., optimized photolithographic processes) combined with IMES sensors on the development tank, UV exposure and oven stages, real stand-by of idle equipment and heaters controlled by takt time. Published evidence and preliminary line observations indicate a potential reduction of 10–15% in the consumption of this stage.
- Reflow/wave soldering, the most energy-intensive stage: an IMES can adjust the thermal profile in real time to avoid overheating, shorten the time needed to reach peak temperature and optimize the operation of frequency-controlled fans; the estimated reduction in oven energy consumption is 12–18% [15,16].
- Automated test benches, which preliminary observations of the line indicate may account for 20–30% of its total energy consumption (an order-of-magnitude estimate, not a metered share): controlled stand-by, automatic shutdown during non-production periods and intelligent management of test-bench lighting target this consumption directly [14].

Table 1 summarizes the savings that a well-implemented IMES is expected to deliver in each area. The values are projections derived from the cited literature and from preliminary observations of the line; they were not obtained from before/after metering of the studied line, and they are therefore not reported as results in Section 3.

Table 1. Estimated energy savings by optimized process area (literature-based projections, not measured on the studied line).

Optimized Area	Projected Savings
Thermal processes (furnaces)	15–20%
Final testing	10–15%
Automatic assembly	8–12%
Stand-by machinery	20–40%

The IMES is intended to operate within an ISO 50001 energy management system [8]. Table 2 maps the elements of ISO 50001:2018 that the proposed architecture would implement on this line, together with the status of each element in the present study. The energy performance indicators and the energy baseline follow the guidance of ISO 50006 [43],

and the verification of any claimed saving would follow the measurement and verification principles of ISO 50015 [44].

Table 2. ISO 50001:2018 elements intended for integration with the IMES architecture and their status in this study.

ISO 50001 Element (Clause)	Implementation in the IMES Architecture	Status in This Study
Energy review and significant energy uses (6.3)	Stage-level metering to rank reflow/wave soldering, PCB thermal processes and test-bench stand-by as significant energy uses	Identified qualitatively (Section 2.2)
Energy performance indicators (6.4)	Energy per conforming unit (Equation (1)); oven energy per panel; stand-by power per test bench	Defined; not yet measured
Energy baseline (6.5)	Pre-IMES consumption normalized to production volume and product mix [43]	Not yet established
Energy data collection plan; monitoring, measurement and analysis (6.6, 9.1)	IMES sensors and the data-acquisition layer shared with the test benches	Architecture in place (Figure 3)
Operational planning and control (8.1)	Takt-controlled heaters, controlled stand-by and automatic shutdown	Proposed (Table 1)
Design and procurement (8.2, 8.3)	Energy criteria for new ovens and test benches	Recommended
Management review and continual improvement (9.3, 10.2)	Periodic joint review of EnPIs and calibration/quality KPIs; verification of savings [44]	Recommended

To link the energy and quality dimensions quantitatively, the following energy performance indicator per conforming unit is proposed for future metering campaigns:

$$E_{CU} = [\Sigma_k E_k + E_T (1 + r_{RT})]/[N (1 - p_S)] \quad (1)$$

where E_k is the metered energy of production stage k, E_T is the energy of first-pass testing of the N units produced in the reference period, r_{RT} is the retest ratio (retests per tested unit), and p_S is the fraction of units scrapped or rejected. The indicator captures how test alerts (through r_{RT}) and tolerance decisions (through p_S) affect the energy cost of each conforming unit; it is discussed in Section 4.

2.3. Correction-Factor Calibration Experiment

A correction factor (CF) is a numerical term applied to the raw output of a sensor to bring its indication as close as possible to the reference value. Every sensor exhibits an internal offset, non-linearity, sensitivity variation and electronic drift; because these effects are largely systematic and stable over time, they can be compensated by a correction, in the sense of the International Vocabulary of Metrology [45]. In the test software, the CF is a numerical multiplier applied to the raw channel output during calibration; the relative increase of about 1% observed for a CF step of 0.01 (Section 3.1) is consistent with a gain term of the form (1 + CF).

The product under investigation (PN 43401) was evaluated on two independent calibration test benches, NEST 1 and NEST 2, each equipped with a light-simulation module (calibrated light source, optical filters, diffusers/collimators), a rain-simulation module

(droplet-pattern and flow-rate control, heating/cooling) and a positioning, power and interface stand communicating with dedicated test-control and data-acquisition software (Figure 4). ChA and ChB readings are the raw digital outputs of the two photodiode paths, expressed in dimensionless signal units (hereafter counts); the expected working range is 36,000–42,000 counts. Table 3 lists the reference (target) values of each bench.

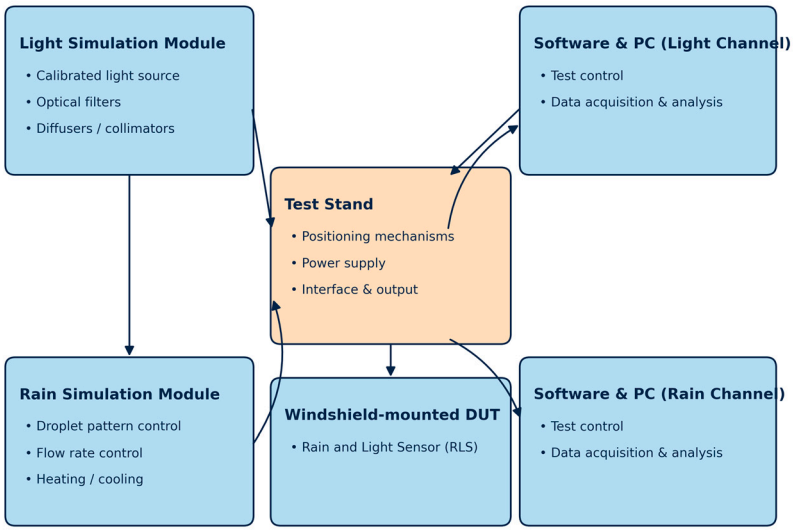


Figure 4. Functional block diagram of the test system for automotive rain and light sensors. Functional block diagram of the test system for automotive rain and light sensors. Arrows indicate the flow of signals and data between modules; the test stand is shown in orange and the simulation modules, the device under test and the test software in blue.

Table 3. Reference (target) calibration values used for NEST 1 and NEST 2.

Bench	Channel	Reference Value (Counts)
NEST 1	Channel A	37,899
NEST 1	Channel B	37,521
NEST 2	Channel A	38,008
NEST 2	Channel B	37,204

Two studies were carried out. In Study 1 (NEST 1, test rigs RT2 and RT5), the CF was first kept constant and then modified, and the relative variation in the channel readings was recorded over ten consecutive test points to establish the baseline consistency of the set-up; no abnormal drift was observed. In Study 2 (NEST 2), ten paired test iterations were performed under identical conditions at CF = 0.02 (initial value; Table 4) and CF = 0.03 (modified value; Table 5); each iteration was repeated after the CF change, so that every pair of readings (e.g., test 1: ChA 36,155 → 36,433 counts) refers to the same test position. For each iteration, the increases ΔChA and ΔChB were computed (Table 6).

Table 4. NEST 2 light-transmission readings, rig RT5, PN 43401, initial correction factor (CF = 0.02).

Test No.	CF	Min (Counts)	ChA (Counts)	ChB (Counts)	Max (Counts)
1	0.02	36,000	36,155	36,241	42,000
2	0.02	36,000	35,983	36,426	42,000
3	0.02	36,000	35,975	36,383	42,000

Table 4. *Cont.*

Test No.	CF	Min (Counts)	ChA (Counts)	ChB (Counts)	Max (Counts)
4	0.02	36,000	36,045	36,263	42,000
5	0.02	36,000	35,828	36,240	42,000
6	0.02	36,000	35,961	36,048	42,000
7	0.02	36,000	36,378	34,992	42,000
8	0.02	36,000	35,974	36,360	42,000
9	0.02	36,000	35,052	36,606	42,000
10	0.02	36,000	35,959	36,766	42,000

Table 5. NEST 2 light-transmission readings, rig RT5, PN 43401, modified correction factor (CF = 0.03).

Test No.	CF	Min (Counts)	ChA (Counts)	ChB (Counts)	Max (Counts)
1	0.03	36,000	36,433	36,571	42,000
2	0.03	36,000	36,291	36,747	42,000
3	0.03	36,000	36,269	36,740	42,000
4	0.03	36,000	36,420	36,688	42,000
5	0.03	36,000	36,110	36,662	42,000
6	0.03	36,000	36,289	36,464	42,000
7	0.03	36,000	36,652	35,319	42,000
8	0.03	36,000	36,289	36,726	42,000
9	0.03	36,000	35,307	36,962	42,000
10	0.03	36,000	36,285	37,167	42,000

Table 6. Per-iteration increase in signal (ΔChA, ΔChB) after the correction-factor adjustment (Table 5 − Table 4).

Test No.	ΔChA (Counts)	ΔChB (Counts)
1	278	330
2	308	321
3	294	357
4	375	425
5	282	422
6	328	416
7	274	327
8	315	366
9	255	356
10	326	401

The general requirements applied to the RLS test benches were: (i) the sensors must be testable according to the functional requirements specified by the stand manufacturer; (ii) the stand must guarantee repeatability, with a maximum variation of 2% between identical test rounds; (iii) all measurements and calibrations must be traceable; (iv) the stand must power and communicate with the sensors via LIN, CAN, I2C or UART, depending on the model; and (v) the system must record both processed parameters and raw data (ChA, ChB, ChC and rain level, among others). The test software performed data acquisition, logging of raw ChA/ChB values, application of the CF, statistical analysis and automatic report generation.

For each CF setting and channel, the mean and the sample standard deviation (SD, $n - 1$ denominator) were computed from the ten readings. The CF effect was assessed with a two-tailed paired-samples t-test on the ten per-iteration differences ($\alpha = 0.05$, 9 degrees of freedom), and the 95% confidence interval (CI) of the mean difference was calculated

with $t_{0.975,\,9} = 2.262$ [46]. The relative change was expressed with respect to the mean at CF = 0.02. A full uncertainty budget in the sense of the GUM [47] was outside the scope of the study; the SD of the paired differences is used here as a measure of repeatability.

2.4. End-of-Line Test System and Automated Test-Log Analysis

A second, independent dataset was obtained from the automated EOL validation of the RLS for the MQB platform (customer part number 17042368-01). Eight production units from a single validation batch (serial numbers 10473753–10473768) were tested in September 2024; the complete EOL sequence for the eight units took approximately five minutes. This dataset therefore precedes the January–September 2025 test-log extracts. The test system communicates with the sensor through LIN [42], with the supply voltage held between 13.3 and 13.7 V; the wake-up current (10–45 mA) and the stand-by (sleep) current (0–0.09 mA) are monitored to confirm that stand-by consumption does not drain the vehicle battery when the engine is off.

The parameters evaluated at EOL, with their units and meaning, are listed in Section 3.3. Light detection uses the forward and global channels, each characterized by an alpha (α) and a beta (β) calibration parameter. These parameters define the calibration curve of each channel; they are computed by the sensor's calibration algorithm to compensate for production variation and ambient conditions and are reported as dimensionless values in the sensor's internal units. Analog-to-digital converter (ADC) linearity is checked at five reference levels and digital-to-analog converter (DAC) linearity at five digital codes (0x00, 0x40, 0x80, 0xC0 and 0xFF); the two trans-impedance amplifier channels (TIA A and TIA B) are evaluated at four of these levels. Environmental compensation is validated through the internal temperature reading (raw counts; stability required within 10 counts) and through the humidity reading (0.001–5%, used for dew-point monitoring to prevent condensation). Final acceptance is based on seven EOL scenarios (three basic-functionality and four advanced-performance tests), whose calculated results for the left and right optical paths (EOL result left/right, dimensionless) must not exceed a safety limit of 2000, and on two families of positional-calibration deviations: left–right (LR) deviations, nominally within 0 to 1.0 (LR #4: −5.0 to 1.0), and global-left/global-right (GS-L/GS-R) deviations, nominally within −1.0 to 1.0. Both deviation families are dimensionless values computed by the EOL software (Microsoft Excel 365, Microsoft Corp., Redmond, WA, USA" or the actual tool) from the positional calibration of the optical paths.

In addition, the automated test logs of two production test rigs, RT2 and RT5, were analyzed at two points of the monitoring period (January 2025 and September 2025). Each record is tagged automatically with the test step at which it was generated (e.g., wake-up current check, DAC/ADC value, optical-amplitude adjustment, LIN communication) and, where applicable, with a functional category (e.g., rain-simulation amplitude adjustment, contact pin, connector/transmission, PCB-assembly rework). Records were aggregated by category, and the categories were ranked by their share of all records, following the Pareto logic commonly used in automotive quality improvement [34]. A flagged record is an alert raised by the test software at a given step; it is not a confirmed physical failure, and alert counts are therefore not equivalent to defect or field-failure rates [48].

3. Results

This section reports measured data only: the CF experiment (Section 3.1), the automated test logs (Section 3.2) and the EOL records (Section 3.3). The energy-saving figures in Table 1 are literature-based projections and are not results of this study; no before/after energy metering of the line was available.

3.1. Effect of the Correction Factor on Light-Transmission Readings

Across the ten paired iterations on NEST 2, raising the CF from 0.02 to 0.03 increased the reading in every case for both channels (Table 6). The mean rose from 35,931.0 to 36,234.5 counts on ChA (+303.5 counts, +0.84%) and from 36,232.5 to 36,604.6 counts on ChB (+372.1 counts, +1.03%) (Table 7). The paired *t*-test showed that the increase is systematic (ChA: $t(9) = 27.7$; ChB: $t(9) = 28.8$; both $p < 0.001$), and the SD of the paired differences (34.6 and 40.8 counts) is about one order of magnitude smaller than the mean shift. These results establish a consistent, monotonic response between the two tested CF levels; with only two levels, they do not establish the shape (linear or otherwise) of the response.

Table 7. Summary statistics of the CF experiment, NEST 2 ($n = 10$ paired iterations per channel).

Channel	Mean (SD), CF = 0.02	Mean (SD), CF = 0.03	Mean Δ (SD)	95% CI of Δ	Relative Change	$t(9)$; p
ChA	35,931.0 (342.3)	36,234.5 (355.4)	303.5 (34.6)	278.7–328.3	+0.84%	27.7; <0.001
ChB	36,232.5 (480.1)	36,604.6 (492.3)	372.1 (40.8)	342.9–401.3	+1.03%	28.8; <0.001

All values in counts except relative change. SD: sample standard deviation ($n - 1$). CI: confidence interval.

The CF change also affected conformity with the working range and the distance from the bench reference values. At CF = 0.02, seven of the ten ChA readings were below the 36,000-count minimum, compared with one at CF = 0.03 (iteration 9); ChB had one reading below the minimum at both settings (iteration 7). Relative to the NEST 2 reference values (Table 3), the mean ChA reading moved from 5.5% to 4.7% below the reference and the mean ChB reading from 2.6% to 1.6% below it.

Two iterations show channel-specific low readings that recur at both CF settings (Figure 5). In iteration 7, ChB was low (34,992 and 35,319 counts) while ChA was at its highest value; in iteration 9, ChA was low (35,052 and 35,307 counts) while ChB was normal. Because each low reading recurs at the same iteration under both CF settings, it affects the absolute signal level but not the CF-related shift, which in iterations 7 and 9 (ΔChB = 327; ΔChA = 255 counts) remains within the range of the other iterations. The interpretation of these readings is discussed in Section 4.

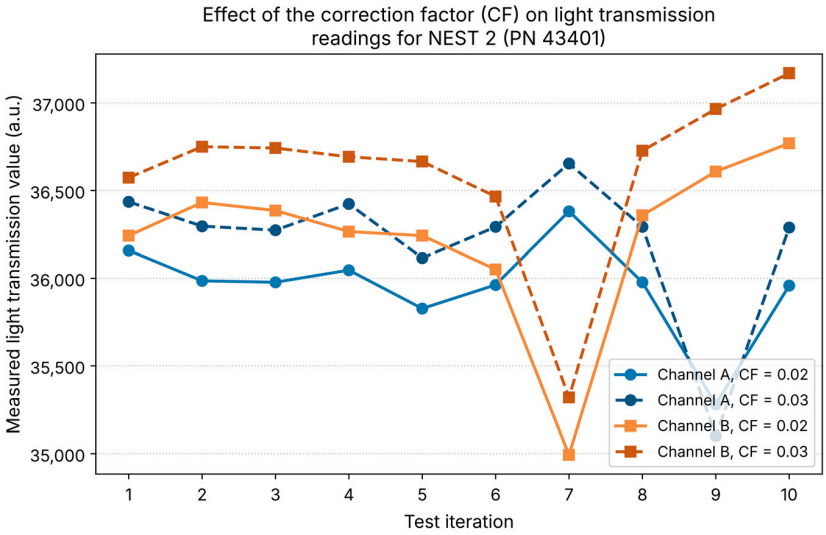


Figure 5. Effect of the correction factor (CF) on light-transmission readings for NEST 2 (PN 43401).

For the NEST 1 baseline study (Study 1), the records show that ChA and ChB fluctuated slightly over the ten consecutive test points without abnormal drift; the individual CF

readings of this study are not available for statistical analysis, so a numerical comparison of the CF effect between the benches cannot be made. The automated test logs, however, record the bench on which each alert was raised, which allows an independent comparison of NEST 1 and NEST 2 (Table 8). The two benches raised similar numbers of alerts at RT5 in both periods (75 versus 86 in January 2025 and 59 versus 56 in September 2025). At RT2, the January 2025 excess on NEST 2 (522 versus 164 alerts) is explained entirely by the rain-simulation amplitude-adjustment step, all 393 of whose alerts were raised on NEST 2; in September 2025 the balance reversed (78 versus 14), with the device-error and Channel-A FFT alerts (21 each) all raised on NEST 1. Bench-specific alert clusters of this kind point to fixture- or bench-related causes rather than to the products tested.

Table 8. Distribution of automated test-log alerts between the two test benches.

Rig	Period	Alerts on NEST 1	Alerts on NEST 2	Total Alerts	Main Bench-Specific Cluster
RT2	January 2025	164	522	686	Rain-simulation amplitude adjustment: 0 on NEST 1, 393 on NEST 2
RT5	January 2025	75	86	161	None (temperature-compensation voltage: 22 vs. 28)
RT2	September 2025	78	14	92	Device error and Channel-A FFT: 21 each on NEST 1, 0 on NEST 2
RT5	September 2025	59	56	115	Channel-B DAC calibration: 30 vs. 17
RT5	Separate extract (Section 3.2)	46	43	89	None

Record totals per bench were not available, so alert shares per bench cannot be computed. Alerts are test-step flags, not confirmed failures.

3.2. Automated Test-Log Analysis

At both rigs and in both periods, most automated test records (87.4–98.2%) carried no alert (Table 9). At RT2, the dominant alert category in January 2025 was the rain-simulation amplitude-adjustment step (7.2% of all records); by September 2025 its share had fallen below 1%, and the remaining alerts were spread over device-error and Channel-A FFT checks (0.4% each). At RT5, alerts remained a small minority of records (3.3% in January and 6.1% in September), dominated first by temperature/humidity-compensation voltage checks and later by Channel-B DAC calibration checks. Within a separate RT5 extract broken down by calibration parameter (Table 10), DAC-value alerts on Channel A account for the largest single share (3.35% of all records). These shares describe how often the software flagged a test step; the number of units that were ultimately defective cannot be derived from them.

Table 9. Summary of automated test-log records by test rig and period.

Rig	Period	Total Records	No Alert	Dominant Alert Category (Share)	Remaining Alerts
RT2	Jan 2025	5436	4750 (87.4%)	Rain-simulation amplitude adjustment, 393 (7.2%)	293 (5.4%): mainly connector, contact-pin and part-number checks, each <1.2%
RT5	Jan 2025	4896	4735 (96.7%)	Temperature-compensation voltage (Tau), 50 (1.0%)	111 (2.3%): mainly humidity-compensation, DAC-value and wake-up-current checks, each <0.8%

Table 9. *Cont.*

Rig	Period	Total Records	No Alert	Dominant Alert Category (Share)	Remaining Alerts
RT2	Sep 2025	5203	5111 (98.2%)	Device error and Channel-A FFT check, 21 each (0.4%)	50 (1.0%): mainly DAC-value, slope and wake-up-current checks, each <0.3%
RT5	Sep 2025	1896	1781 (93.9%)	Channel-B DAC calibration (S2 DAC ChB G1), 47 (2.5%)	68 (3.6%): mainly FFT, customer H/L pin, DAC-value and communication checks, each <0.8%

Alert counts are test-step flags raised by the test software, not confirmed failures or field-failure rates.

Table 10. RT5 test rig: distribution of alerts by calibration parameter.

Alert Category	Count	Share of Total
MQB Channel A DAC value	60	3.35%
MQB Channel B DAC value	12	0.67%
MQB Channel A slope	9	0.50%
MQB Channel B slope	5	0.28%
Customer software version	2	0.11%
LIN/contact/fixture (Anlage) check	1	0.06%
No alert	1700	95.03%
Total	1789	100.00%

This RT5 extract (1789 records; 46 alerts on NEST 1 and 43 on NEST 2) is separate from the January and September 2025 extracts summarized in Table 9.

3.3. End-of-Line Deviation and Specification Analysis

All eight EOL-tested units passed the pass/fail criterion (FailureCode = 0.0), and the ADC/DAC linearity and TIA channel results were within their specification bands, indicating a well-controlled amplification stage. However, several of the eight units showed positional-calibration deviations well outside the nominal ±1.0 tolerance: LR deviations of up to ±36.9 against a 0 to 1.0 band, and GS-L/GS-R deviations of up to ±38.5 against a −1.0 to 1.0 band (Table 11). Since these units nevertheless passed, the LR and GS-L/GS-R deviations are evidently recorded and monitored at EOL but are not part of the automated pass/fail decision. With all other EOL parameters within specification, the deviations most likely reflect either a nominal tolerance that is tight relative to the natural variability of the optical alignment process, or a localized source of variation in the alignment step (e.g., fixture wear or windshield-mounting variability), rather than a generalized fault of the sensor electronics.

Table 11. RLS calibration and specification parameters at EOL: units, nominal ranges and measured values (eight units, PN 17042368-01, September 2024).

Parameter	Unit	Specification/Nominal Range	Measured Range
Alpha (α), forward channel	Dimensionless	—	−870 to −1120
Beta (β), forward channel	Dimensionless	—	1310 to 1630
Alpha (α), global channel	Dimensionless	—	−900 to −1140
Beta (β), global channel	Dimensionless	—	980 to 1300

Table 11. *Cont.*

Parameter	Unit	Specification/Nominal Range	Measured Range
ADC test result, levels 0–4	Counts	3712–4480; 16,000–16,768; 48,768–49,536; 61,056–61,824; 30,984–35,152	Within specification
TIA amplifier, Channel A	Counts	—	35,442–35,981
TIA amplifier, Channel B	Counts	—	35,486–35,808
Wake-up current	mA	10–45	Within specification
Stand-by (sleep) current	mA	0–0.09	Within specification
Supply voltage (LIN)	V	13.3–13.7	Within specification
Internal temperature reading	Counts	10,000–15,000; stability < 10	Within specification
Sensor operating temperature	°C	20–35	Within specification
Humidity reading (dew-point monitoring)	%	0.001–5	Within specification
EOL result, left/right (7 scenarios)	Dimensionless	≤2000 (safety limit)	200–700
Left–right (LR) deviation	Dimensionless	0 to 1.0 (LR #4: −5.0 to 1.0)	Up to ±36.9
Global-left/global-right (GS-L/GS-R) deviation	Dimensionless	−1.0 to 1.0	Up to ±38.5

4. Discussion

The CF experiment shows that raising the correction factor from 0.02 to 0.03 produces a predictable, statistically significant and highly repeatable increase in both channels. Because only two CF levels were tested, the result supports a consistent, monotonic response within the tested range but not a linear calibration curve; sensor behavior at intermediate or more extreme CF values remains untested. If the CF acts as a multiplicative gain, the two channels should respond by similar relative amounts; the larger response of ChB (+1.03% versus +0.84%), consistent across all ten iterations, rather suggests a small difference in optical or electronic gain between the channels. The adjustment moved both channel means closer to the bench reference values, but ChA remained about 4.7% below its reference, which indicates that a single CF step does not fully compensate for the offset of this channel and that the calibration curve should be mapped over a wider CF range. A complete uncertainty budget [47] and a gauge repeatability and reproducibility study across both benches [49] are needed before the calibration algorithm can be claimed to behave uniformly across benches: the NEST 1 baseline showed no abnormal drift, but its CF readings were not available for a numerical comparison. In quality-oriented manufacturing system design, in-line measurement data of this kind are used not only for acceptance decisions but also as feedback for adjusting process and calibration parameters [50], which is the role that the CF plays on the RLS benches; mapping the CF response more completely is therefore a prerequisite for using it as a controlled adjustment rather than as a fixed setting.

The channel-specific low readings in iterations 7 and 9 illustrate a practical problem of automated testing: distinguishing transient measurement glitches from genuine component or fixture defects. In this dataset, each low reading recurred at the same iteration under both CF settings while the other channel remained normal, which points to a reproducible property of the tested item or of its position in the fixture rather than to random electrical

noise, since each pair of readings refers to the same test position (Section 2.3). The bench-specific alert clusters in Table 8, such as the 393 rain-simulation alerts raised only on NEST 2 at RT2 in January 2025, point in the same direction at the level of the production logs. In production, the two cases can be separated by a staged protocol: an immediate retest of the same unit in the same fixture (a transient glitch does not repeat); a retest in a different fixture or on the second bench (a fixture fault follows the fixture, a component defect follows the unit); periodic runs of a golden reference unit at the start of each shift (drift of the bench itself); recording of contact resistance and supply current at the affected step; and control charts of per-position residuals [46]. Recording the outcome of each step allows alerts to be classified as transient, fixture-related or component-related, and avoids the costly no-fault-found cycles described in the maintenance literature [48]. The root causes of such events include intermittent faults, inadequate test procedures or test coverage, and organizational factors [51], all of which are plausible at the affected RLS test steps. Recent work on printed circuit board assemblies has shown that historical inspection and test records can be used to predict the defect rates of new production orders [52]; the classified retest outcomes proposed here could later provide comparable training data for predictive quality models on the RLS line.

The same caution applies to the test-log statistics. The alert shares in Tables 9 and 10 are counts of flagged test steps and are not defect prevalences or field-failure rates: a reading close to a limit can be flagged by measurement variability alone, so that a conforming unit is falsely rejected, a risk that conformity assessment manages through decision rules and guard bands based on measurement uncertainty [53]. The consumer's and producer's risks associated with such decisions can be quantified when the measurement uncertainty is known [54]; more recent work has extended the evaluation of true and false conformity decisions from individual items to whole samples of items [55] and has shown with practical examples how decision rules that account for uncertainty, such as guard banding, shift the balance between false acceptance and false rejection [56]. Applied to the RLS benches, this framework would allow the alert limits of each test step to be set according to an explicit and documented risk of false rejection rather than by convention. Read in this way, the reduction in RT2 rain-simulation amplitude alerts from 7.2% to below 1% between January and September 2025 shows that the step generated fewer flags over time, and because all of these alerts were raised on NEST 2 (Table 8), the change concerned that bench (for example, a correction of its rain-simulation fixture or of the step's limits) rather than the products tested; it does not by itself quantify a reduction in defective output.

The EOL deviations are the most important quality signal in the dataset, but they rest on eight units from a single validation batch. This sample shows that deviations far beyond the nominal tolerance exist and indicates their approximate magnitude, but it cannot support a statistical distribution, a capability estimate or a root-cause inference. For example, even if none of the eight units had exceeded the tolerance, the one-sided 95% upper confidence bound on the proportion of nonconforming units would still be about 31% ($1 - 0.05^{1/8}$); capability indices [57] and statistical tolerance intervals [58] require substantially larger samples drawn from several batches and periods. Reviews of capability analysis further caution that point estimates of capability indices depend on distributional assumptions and are subject to considerable sampling variability [59,60], a caution that applies with particular force to deviations that, as here, may not be normally distributed. The quality findings should therefore be read as a signal that justifies a targeted investigation, not as an estimate of the production nonconformity rate. Two non-exclusive explanations should be tested: that the ± 1.0 tolerance was set without reference to production capability data, and that the deviations arise from assignable causes in the alignment step (specific fixtures,

shifts or component batches). Before either conclusion is drawn, the measurement system itself must be shown to be adequate relative to the tolerance [49].

The deviations also have a functional-safety dimension. A positional deviation between the left and right, or between the global-left and global-right, light measurements biases the sensor's estimate of ambient brightness in a direction-dependent way. In the vehicle, such a bias would shift the effective switching thresholds of the automatic headlamp function: an underestimated darkness delays switching on when entering a tunnel or at dusk, whereas an overestimated darkness causes unnecessary switching. Automatic switching of the dipped beam is a regulated function [17], and where the sensor output feeds ADAS-related lighting functions, such errors fall within the scope of the hazard analysis and risk assessment required by ISO 26262 [61]. The rain channel raises an analogous concern, since a miscalibrated rain signal delays wiper activation and reduces visibility in adverse weather. Translating a deviation of a given size into a switching-threshold error in lux requires the transfer function between the deviation unit and illuminance, which was not available in this study; establishing it is a prerequisite for deciding whether the observed deviations are functionally relevant or whether the tolerance can be relaxed safely.

On the energy side, the projected 15–25% per-unit savings (Table 1) are more conservative than the reductions reported for single-machine IIoT retrofits (56% after correction of a compressed-air leak [11]) and for digital-twin deployments (up to 30% across fifty studies [13]). Longitudinal evidence from 83 ISO 50001-certified manufacturing facilities points in the same direction at a smaller annual scale, with average energy performance improvements of about 4.1% in the first year of implementation and about 3.4% per year twelve years later [62]. Structured on-site energy assessments in 13 U.S. manufacturing plants in 2023–2024 identified 234 operational and maintenance opportunities for reducing energy use and emissions [63], and, for reflow soldering specifically, a recent data-driven recipe-optimization study reported a 23% reduction in oven energy cost while keeping the thermal profile close to its target [64], which suggests that the 12–18% oven saving assumed for this line is a conservative estimate. Whether such savings materialize depends on organizational as well as technical factors: reviews of industrial energy management emphasize responsibilities, practices and continual improvement [65], and a recent analysis of Industry 4.0 technologies found that their main enabling effects on energy management concern awareness, connectivity and integration, and visualization, chiefly by improving energy monitoring and performance evaluation [66]—precisely the functions that the IMES data-acquisition layer is intended to provide. The difference is expected: those figures usually describe a single, previously unmonitored machine or utility system after a specific inefficiency has been diagnosed, whereas Table 1 describes the aggregate effect of continuous monitoring across a mixed electronics/optical line. The projections nevertheless remain projections. Turning them into verified savings requires the ISO 50001 elements listed in Table 2 that are not yet in place—above all, a metered energy baseline normalized to production volume and product mix and a set of EnPIs [43]—followed by measurement and verification of the change [44]. The claim that combining IMES with ISO 50001 practices yields savings above 20% is consistent with the reported effects of ISO 50001 adoption on energy intensity [9,10], but it has to be verified on this line.

The present data do not establish a measured quantitative relationship between the energy management of the switching-module line and the optical calibration of the sensors; the two analyses share the IMES data infrastructure but were carried out on separate datasets. Equation (1) provides the quantitative link to be measured in future work. Its retest term shows how test alerts translate into energy: if every flagged record in Table 9 triggered one retest, the test-stage energy E_T would increase by 1.8–12.6% (the alert shares of the four rig-period combinations), so that halving the alert rate of a rig reduces its

test energy proportionally. Its scrap term shows how tolerance decisions translate into energy: a tolerance that rejects conforming units raises the energy cost of every unit that is shipped. Because the actual retest policy and the energy of each test step were not recorded, these figures are an upper-bound illustration rather than a measurement; they nonetheless show that calibration quality and energy efficiency are coupled through the same production records, in line with the zero-defect manufacturing perspective [36]. This coupling is increasingly recognized in research on sustainable manufacturing. Energy and resource efficiency have been analyzed at both the process and the system level [67], and zero-defect manufacturing has been proposed explicitly as a route to higher manufacturing sustainability, because every defect that is prevented also avoids the energy and materials that would otherwise be spent on it [68]. Subsequent reviews have consolidated its detection, prediction, prevention and repair strategies [69] and extended them with dimensions aimed at sustainable production [70], while comparative modeling studies have evaluated detection–repair, detection–prevention and prediction–prevention strategies against the constraints of different manufacturing set-ups [71]. Within this framework, Equation (1) can be read as a line-level operationalization of zero-defect thinking, in which the retest ratio and the scrap fraction quantify the energy penalty of detection-based quality control.

The proposal to feed IMES energy data and test-log data into predictive-maintenance models is a conceptual direction, not an outcome of this study: no predictive model, feature-engineering pipeline or prediction result was developed. The literature indicates that such models are feasible in principle [30,31] and that energy consumption patterns carry diagnostic information on equipment state [32,33]. Systematic reviews of machine-learning [72] and deep-learning [73] approaches to predictive maintenance, together with recent comparisons of deep-learning models trained on industrial sensor data [74], identify the availability of representative, labeled failure data as a recurrent constraint on model performance; on this line, such labels would first have to be generated by the alert-classification protocol described above. Candidate features for this line include stage-level power profiles, stand-by durations, alert rates per test step and CF-corrected channel residuals; the September 2025 alert shares in Table 9 could serve as an initial baseline. As vehicles become more automated, rain/light sensors will need higher accuracy, faster response and more advanced self-diagnosis, which makes this integration an attractive, though still unvalidated, route to combining quality and energy objectives.

From a sustainability perspective, the study contributes at three levels. At the level of the production line, it identifies where energy can be saved—thermal processes and stand-by of the automated test benches (Table 1)—and specifies, in Table 2, the ISO 50001 elements needed to turn these projections into verified reductions in energy intensity and, depending on the carbon intensity of the electricity supply, in the associated greenhouse-gas emissions [9,10,62]. At the level of the product, it shows that calibration and test decisions carry an environmental cost that is normally invisible in energy accounting: the CF adjustment reduced the number of Channel A readings below the working-range minimum from seven to one (Section 3.1), and each out-of-range reading that is avoided potentially avoids a retest, a rework operation or a rejected unit, together with the energy, materials and handling that it would consume. Equation (1) expresses this effect as a single sustainability indicator, the energy per conforming unit, which increases with every retest (through the retest ratio) and every rejected unit (through the scrap fraction) and therefore rewards quality improvements and energy improvements in the same metric. At the level of the vehicle, a correctly calibrated RLS supports reliable automatic headlamp and wiper operation and hence driver visibility, which links the manufacturing results to the social dimension of sustainability through road safety [17,61].

The approach is transferable to other automotive and electronics lines that combine energy-intensive thermal processes with precision optical or electrical testing. Because Equation (1) uses data that such lines already record—stage-level energy, test outcomes, retests and scrap—it can be calculated without additional instrumentation once IMES metering is in place, and it can be reported alongside the energy performance indicators required by ISO 50001 and in corporate sustainability reporting. In this sense, the study shows how an Industrial Energy Management System can be extended from a tool for controlling energy costs into an instrument for sustainable, resource-efficient production, consistent with the zero-defect manufacturing perspective [36] and with SDGs 9, 12 and 13. These benefits remain conditional on the metering campaign and the follow-up studies listed in Table 12; until then, they are projected rather than measured.

Table 12. Limitations of the study and the corresponding future work.

No.	Limitation	Future Work Addressing It
L1	CF tested at two levels only (0.02 and 0.03), ten pairs, one product (PN 43401); response shape untested.	CF sweep at intermediate and extreme levels (e.g., 0.015–0.040 in 0.005 steps) on several RLS variants, with regression and lack-of-fit testing.
L2	No numerical CF readings from NEST 1; cross-bench comparison limited to alert counts (Table 8).	Cross-bench study with the same units on NEST 1 and NEST 2, including a gauge repeatability and reproducibility study [49].
L3	EOL deviations from eight units of a single batch; no distribution, capability estimate or root cause.	Sampling across several batches and periods; capability indices [57] and tolerance intervals [58]; formal 8D investigation [34]; tolerance review.
L4	Test-log alerts are step flags; transient readings cannot be separated from defects.	Staged retest protocol (same fixture, other fixture or bench, golden unit) with outcome recording and classification of alerts [48].
L5	Functional impact of LR/GS deviations not quantified.	Determination of the transfer function from deviation to switching-threshold error (lux) and assessment against UN R48 and ISO 26262 [17,61].
L6	Energy savings are literature-based projections; no metered baseline.	Metering campaign with energy baseline and EnPIs [43] and measurement and verification of savings [44].
L7	No measured quantitative link between energy and calibration quality.	Monthly calculation of the energy per conforming unit, Equation (1), with recorded retest and scrap data.
L8	Predictive maintenance is conceptual; no model was trained.	Development and prospective validation of a model using energy and test-log features [30,31,33].

Table 12 summarizes the limitations of the study and maps each of them to the follow-up activity that addresses it.

5. Conclusions

This case study examined the energy and quality dimensions of a single MQB-platform line for headlight switching modules and windshield rain/light sensors. On the metrological side, which rests on measured data, raising the optical correction factor from 0.02 to 0.03 increased the light-transmission signal by 0.84% on Channel A and 1.03% on Channel B (paired t-test, $p < 0.001$) in a highly repeatable way, reduced the number of Channel A readings below the working-range minimum from seven to one, and moved both channels closer to their reference values. The response was consistent and monotonic between the two tested levels; its linearity, and its behavior outside this range, remain to be established.

The automated test logs showed that 87.4–98.2% of test records carried no alert, with the remaining alerts concentrated in a few test steps; these shares describe flagged test steps, not defect or field-failure rates. The EOL analysis of eight units revealed left–right and global-light positional deviations far beyond the nominal ±1.0 tolerance, even though all units passed the acceptance criterion. Given the small sample, this finding justifies a tolerance review and a targeted root-cause investigation, including an assessment of the functional impact on automatic headlamp switching, rather than an estimate of the nonconformity rate.

On the energy side, IMES adoption is projected, on the basis of the literature and preliminary line observations, to reduce energy consumption by 15–25% per unit, with the largest opportunities in thermal processes (reflow/wave soldering) and in stand-by management of the automated test benches; combined with ISO 50001 practices, savings above 20% are expected. These are projections, not measured savings, and their verification requires a metered baseline, EnPIs and measurement and verification of the savings within the ISO 50001 framework outlined in Table 2. The proposed energy indicator per conforming unit links the two dimensions: fewer false alerts and better-founded tolerances reduce the energy consumed per shipped unit. Together, these results indicate that IMES adoption can support energy and quality objectives on the same line, provided that the savings are verified by metering and that calibration tolerances and alert categories are reviewed periodically against the accumulated test data. In sustainability terms, the study offers automotive electronics manufacturers a practical route to lowering the energy, material and emission intensity of each conforming unit by managing energy efficiency and calibration quality together rather than as separate objectives.

Author Contributions: Conceptualization, A.I.F., D.D. and O.R.C.; methodology, A.I.F., D.D. and O.R.C.; software, D.D.; validation, A.I.F., D.D. and O.R.C.; formal analysis, C.E.; investigation, D.D.; resources, D.D.; data curation, D.D. and M.G.; writing—original draft preparation, A.Ş.I.; writing—review and editing, A.I.F., D.D., E.P. and O.R.C.; supervision, A.I.F. and O.R.C.; visualization, A.I.F., D.D., E.P. and O.R.C.; project administration, A.I.F., D.D. and O.R.C.; funding acquisition, O.R.C. All authors have read and agreed to the published version of the manuscript.

Funding: This research received no external funding.

Institutional Review Board Statement: Not applicable.

Informed Consent Statement: Not applicable.

Data Availability Statement: The original contributions presented in this study are included in the article. Further inquiries can be directed to the corresponding authors.

Conflicts of Interest: The authors declare no conflicts of interest.

Abbreviations

The following abbreviations are used in this manuscript:

8D	Eight disciplines (problem-solving method)
ADAS	Advanced driver-assistance systems
ADC	Analog-to-digital converter
CF	Correction factor
ChA, ChB	Channel A (forward), Channel B (global)
CI	Confidence interval
DAC	Digital-to-analog converter
DMAIC	Define–Measure–Analyze–Improve–Control
ECU	Electronic control unit
EnPI	Energy performance indicator

EOL	End of line
FMEA	Failure mode and effects analysis
GS-L/GS-R	Global-left/global-right (deviation)
IIoT	Industrial Internet of Things
IMES	Industrial Energy Management System
KPI	Key performance indicator
LIN	Local Interconnect Network
LR	Left–right (deviation)
MQB	Modularer Querbaukasten (modular transverse toolkit)
NEST 1, NEST 2	Calibration test benches
PCB	Printed circuit board
PN	Part number
RAMS	Reliability, availability, maintainability and safety
RLS	Rain/light sensor
RT2, RT5	Production test rigs
SD	Standard deviation
TIA	Trans-impedance amplifier

References

1. Bunse, K.; Vodicka, M.; Schönsleben, P.; Brülhart, M.; Ernst, F.O. Integrating Energy Efficiency Performance in Production Management—Gap Analysis between Industrial Needs and Scientific Literature. *J. Clean. Prod.* **2011**, *19*, 667–679. [CrossRef]
2. May, G.; Taisch, M.; Prabhu, V.V.; Barletta, I. Energy Related Key Performance Indicators—State of the Art, Gaps and Industrial Needs. In *Advances in Production Management Systems. Sustainable Production and Service Supply Chains (APMS 2013)*; IFIP Advances in Information and Communication Technology; Springer: Berlin/Heidelberg, Germany, 2013; Volume 414, pp. 257–267. [CrossRef]
3. May, G.; Barletta, I.; Stahl, B.; Taisch, M. Energy Management in Production: A Novel Method to Develop Key Performance Indicators for Improving Energy Efficiency. *Appl. Energy* **2015**, *149*, 46–61. [CrossRef]
4. Noronha, F.H.d.S.; Cisneros, E.A.G.; Munhoz, D.L.d.S.; Printes, A.L.; Chuquitaipe, E.A.N.; Silva, J.; Sales, M.d.L.B. Maintenance of Automated Production Lines in Industry through the Application of Indicators. *GeSec* **2025**, *16*, e5127. [CrossRef]
5. Brunzini, A.; Micucci, F.M.; Cappelletti, F.; Rossi, M.; Germani, M. Performance Monitoring and Optimization of Robotic Production Lines: A Granular Approach for a KPIs-Based Study in Industrial Automation. In Proceedings of the ASME 2024 International Mechanical Engineering Congress and Exposition (IMECE2024), Portland, OR, USA, 17–21 November 2024. [CrossRef]
6. Raza, T.; Muhammad, M.; Majid, M.A.A. A Comprehensive Framework and Key Performance Indicators for Maintenance Performance Measurement. *ARPN J. Eng. Appl. Sci.* **2016**, *11*, 12146–12152.
7. Cinar, E.; Kalay, S.; Sarıçiçek, İ. A Predictive Maintenance System Design and Implementation for Intelligent Manufacturing. *Machines* **2022**, *10*, 1006. [CrossRef]
8. *ISO 50001:2018*; Energy Management Systems—Requirements with Guidance for Use. International Organization for Standardization: Geneva, Switzerland, 2018.
9. Wang, E.-Z.; Pan, T. Does ISO 50001 Adoption Reduce Manufacturing Energy Intensity? Micro-Evidence from China. *Econ. Anal. Policy* **2025**, *86*, 653–672. [CrossRef]
10. McKane, A.T.; Therkelsen, P.L.; Scodel, A.; Rao, P.; Aghajanzadeh, A.; Hirzel, S.; Zhang, R.; Prem, R.; Fossa, A.; Lazarevska, A.M.; et al. Predicting the Quantifiable Impacts of ISO 50001 on Climate Change Mitigation. *Energy Policy* **2017**, *107*, 278–288. [CrossRef]
11. Hanifi, S.; Alkali, B.; Lindsay, G.; McGlinchey, D. Optimizing Energy and Air Consumption in Smart Manufacturing: An Industrial Internet of Things-Based Monitoring and Efficiency Enhancement Solution. *Appl. Sci.* **2025**, *15*, 3222. [CrossRef]
12. Xia, T.; Sun, H.; Ding, Y.; Han, D.; Qin, W.; Seidelmann, J.; Xi, L. Digital Twin-Based Real-Time Energy Optimization Method for Production Line Considering Fault Disturbances. *J. Intell. Manuf.* **2025**, *36*, 569–593. [CrossRef]
13. Ba, L.; Tangour, F.; El Abbassi, I.; Absi, R. Analysis of Digital Twin Applications in Energy Efficiency: A Systematic Review. *Sustainability* **2025**, *17*, 3560. [CrossRef]
14. Mouzon, G.; Yildirim, M.B.; Twomey, J. Operational Methods for Minimization of Energy Consumption of Manufacturing Equipment. *Int. J. Prod. Res.* **2007**, *45*, 4247–4271. [CrossRef]
15. Esfandyari, A.; Kreitlein, S.; Schmidt, E.; Franke, J. Thermodynamic and Theoretical-Based Modeling and Assessment of an Energy-Efficient Performance Measurement System in the Soldering Process. In Proceedings of the 2016 Electronics Goes Green 2016+ (EGG), Berlin, Germany, 6–9 September 2016; pp. 1–6. [CrossRef]

16. Esfandyari, A.; Javied, T.; Reissmann, F.; Franke, J. A Standby Strategy Model for an Energy Efficient Soldering Oven Machine. In Proceedings of the 2016 IEEE Conference on Technologies for Sustainability (SusTech), Phoenix, AZ, USA, 9–11 October 2016; pp. 47–51. [CrossRef]
17. *UN Regulation No. 48*; Uniform Provisions Concerning the Approval of Vehicles with Regard to the Installation of Lighting and Light-Signalling Devices. United Nations Economic Commission for Europe (UNECE): Geneva, Switzerland, 1982.
18. Supriya, K.E.; Kanchi, R.R. Real Time Rain Sensing and Wind Shield Wiper Control System with Cloud Computing and Geotagging Applications. *Int. J. Inf. Technol.* **2020**, *12*, 839–847. [CrossRef]
19. Szkoda, M.; Kaczor, G.; Satora, M. Methodology of Building the Strategy of Maintenance of Rail Vehicles with the Use of the RAMS Analysis in the Area of Safety. *J. KONBiN* **2019**, *49*, 219–244. [CrossRef]
20. Hidirov, S.; Guler, H. Railway Infrastructure Reliability, Availability, Maintainability and Safety (RAMS) Analysis. In Proceedings of the International Symposium on Innovative Technologies in Engineering and Science (ISITES), Baku, Azerbaijan, 29 September–1 October 2017.
21. Praticò, F.G.; Giunta, M. An Integrative Approach RAMS–LCC to Support Decision on Design and Maintenance of Rail Track. In Proceedings of the 10th International Conference Environmental Engineering, Vilnius, Lithuania, 27–28 April 2017. [CrossRef]
22. Guck, D.; Katoen, J.P.; Stoelinga, M.; Luiten, T.; Romijn, J. Smart Railroad Maintenance Engineering with Stochastic Model Checking. In Proceedings of the Second International Conference on Railway Technology, Ajaccio, France, 8–11 April 2014. [CrossRef]
23. Patra, A.P. Maintenance Decision Support Models for Railway Infrastructure Using RAMS and LCC Analyses. Doctoral Dissertation, Luleå University of Technology, Luleå, Sweden, 2009.
24. Li, G.; Yi, L.; Zhang, X.; Chao, H.; He, J.; Xu, B.; Jinghao, C. Development of a Preventive Maintenance Strategy for an Automatic Production Line Based on Group Maintenance Method. *Appl. Sci.* **2018**, *8*, 1781. [CrossRef]
25. Lyu, W.; Zhang, X.; Fan, Y. Cost-Reliability Based Group Maintenance Model for Automatic Production Line. *Comput. Integr. Manuf. Syst.* **2013**, *19*, 2954–2959. [CrossRef]
26. Yang, M.; Li, C.; Tang, Y.; Xiong, M. Availability-Oriented Maintenance Strategy of Key Equipment in Automated Production Line Considering Performance Degradation. *IEEE Robot. Autom. Lett.* **2023**, *8*, 3182–3189. [CrossRef]
27. Olivotti, D.; Passlick, J.; Dreyer, S.; Lebek, B.; Breitner, M.H. Maintenance Planning Using Condition Monitoring Data. In *Operations Research Proceedings 2017*; Springer: Cham, Switzerland, 2018; pp. 543–548. [CrossRef]
28. Tian, Z.; Wu, B.; Chen, M. Condition-Based Maintenance Optimization Considering Improving Prediction Accuracy. *J. Oper. Res. Soc.* **2014**, *65*, 1412–1422. [CrossRef]
29. Truong-Ba, H.; Borghesani, P.; Cholette, M.E.; Ma, L. Optimization of Condition-Based Maintenance Considering Partial Opportunities. *Qual. Reliab. Eng. Int.* **2020**, *36*, 529–546. [CrossRef]
30. Zonta, T.; da Costa, C.A.; da Rosa Righi, R.; Lima, M.J.; da Trindade, E.S.; Li, G.-P. Predictive Maintenance in the Industry 4.0: A Systematic Literature Review. *Comput. Ind. Eng.* **2020**, *150*, 106889. [CrossRef]
31. Arez, D.; Navas, H.V.G.; Gaspar, P. The Bridge Between Artificial Intelligence and Predictive Maintenance in Industry 4.0: A Systematic Review. *Appl. Sci.* **2026**, *16*, 4882. [CrossRef]
32. Faltinski, S.; Flatt, H.; Pethig, F.; Kroll, B.; Vodenčarević, A.; Maier, A.; Niggemann, O. Detecting Anomalous Energy Consumptions in Distributed Manufacturing Systems. In Proceedings of the 10th IEEE International Conference on Industrial Informatics (INDIN), Beijing, China, 25–27 July 2012; pp. 358–363. [CrossRef]
33. Mendia, I.; Gil-Lopez, S.; Grau, I.; Del Ser, J. A Novel Approach for the Detection of Anomalous Energy Consumption Patterns in Industrial Cyber-Physical Systems. *Expert Syst.* **2024**, *41*, e12959. [CrossRef]
34. Škůrková, K.L.; Fidlerová, H.; Niciejewska, M.; Idzikowski, A. Quality Improvement of the Forging Process Using Pareto Analysis and 8D Methodology in Automotive Manufacturing: A Case Study. *Standards* **2023**, *3*, 84–94. [CrossRef]
35. Jou, Y.-T.; Silitonga, R.M.; Lin, M.-C.; Sukwadi, R.; Rivaldo, J. Application of Six Sigma Methodology in an Automotive Manufacturing Company: A Case Study. *Sustainability* **2022**, *14*, 14497. [CrossRef]
36. Psarommatis, F.; May, G.; Dreyfus, P.-A.; Kiritsis, D. Zero Defect Manufacturing: State-of-the-Art Review, Shortcomings and Future Directions in Research. *Int. J. Prod. Res.* **2020**, *58*, 1–17. [CrossRef]
37. Nioata, A.; Ţăpirdea, A.; Chivu, O.R.; Feier, A.; Enache, I.C.; Gheorghe, M.; Borda, C. Workplace Safety in Industry 4.0 and Beyond: A Case Study on Risk Reduction Through Smart Manufacturing Systems in the Automotive Sector. *Safety* **2025**, *11*, 50. [CrossRef]
38. Rînjea, C.; Chivu, O.R.; Darabont, D.-C.; Feier, A.I.; Borda, C.; Gheorghe, M.; Nitoi, D.F. Influence of the Thermal Environment on Occupational Health and Safety in Automotive Industry: A Case Study. *Int. J. Environ. Res. Public Health* **2022**, *19*, 8572. [CrossRef] [PubMed]
39. Barbu, A.; Feier, A.I.; Petzek, E.; Gheorghe, M. Investigation of a Composite Material Painting Method: Assessment of the Mixture Curing of Organic Coatings. *Processes* **2025**, *13*, 2394. [CrossRef]
40. Hecht, E. *Optics*, 5th ed.; Pearson: Boston, MA, USA, 2017.

41. *ISO/CIE 23539:2023*; Photometry—The CIE System of Physical Photometry. International Organization for Standardization: Geneva, Switzerland, 2023.
42. *ISO 17987-1:2016*; Road Vehicles—Local Interconnect Network (LIN)—Part 1: General Information and Use Case Definition. International Organization for Standardization: Geneva, Switzerland, 2016.
43. *ISO 50006:2023*; Energy Management Systems—Evaluating Energy Performance Using Energy Performance Indicators and Energy Baselines. International Organization for Standardization: Geneva, Switzerland, 2023.
44. *ISO 50015:2014*; Energy Management Systems—Measurement and Verification of Energy Performance of Organizations—General Principles and Guidance. International Organization for Standardization: Geneva, Switzerland, 2014.
45. *JCGM 200:2012*; International Vocabulary of Metrology—Basic and General Concepts and Associated Terms (VIM). 3rd ed. Joint Committee for Guides in Metrology: Sèvres, France, 2012.
46. Montgomery, D.C. *Introduction to Statistical Quality Control*, 8th ed.; Wiley: Hoboken, NJ, USA, 2019.
47. *JCGM 100:2008*; Evaluation of Measurement Data—Guide to the Expression of Uncertainty in Measurement. Joint Committee for Guides in Metrology: Sèvres, France, 2008.
48. Khan, S.; Phillips, P.; Jennions, I.; Hockley, C. No Fault Found Events in Maintenance Engineering Part 1: Current Trends, Implications and Organizational Practices. *Reliab. Eng. Syst. Saf.* **2014**, *123*, 183–195. [CrossRef]
49. Automotive Industry Action Group (AIAG). *Measurement Systems Analysis (MSA) Reference Manual*, 4th ed.; AIAG: Southfield, MI, USA, 2010.
50. Colledani, M.; Tolio, T.; Fischer, A.; Iung, B.; Lanza, G.; Schmitt, R.; Váncza, J. Design and Management of Manufacturing Systems for Production Quality. *CIRP Ann.* **2014**, *63*, 773–796. [CrossRef]
51. Khan, S.; Phillips, P.; Hockley, C.; Jennions, I. No Fault Found Events in Maintenance Engineering Part 2: Root Causes, Technical Developments and Future Research. *Reliab. Eng. Syst. Saf.* **2014**, *123*, 196–208. [CrossRef]
52. Miedema, E.; Kortman, H.; Emmanouilidis, C. Predicting Defect Rates of Printed Circuit Board Assemblies: Towards Zero Defect Manufacturing and Zero-Maintenance Strategies. *IFAC-PapersOnLine* **2024**, *58*, 91–96. [CrossRef]
53. *JCGM 106:2012*; Evaluation of Measurement Data—The Role of Measurement Uncertainty in Conformity Assessment. Joint Committee for Guides in Metrology: Sèvres, France, 2012.
54. Pendrill, L.R. Using Measurement Uncertainty in Decision-Making and Conformity Assessment. *Metrologia* **2014**, *51*, S206–S218. [CrossRef]
55. Pennecchi, F.; Kuselman, I. Probabilities of True and False Decisions in Conformity Assessment of a Finite Sample of Items. *Meas. Sci. Technol.* **2024**, *35*, 056003. [CrossRef]
56. Carullo, A.; Manta, F.; Mugno, R.; Paolino, E.; Pedone, P.; Albis, G.; Corbellini, S.; Vallan, A. Fundamentals in Measurement: The Role of Measurement Uncertainty in Conformity Assessment: Some Examples. *IEEE Instrum. Meas. Mag.* **2024**, *27*, 5–12. [CrossRef]
57. Kane, V.E. Process Capability Indices. *J. Qual. Technol.* **1986**, *18*, 41–52. [CrossRef]
58. *ISO 16269-6:2014*; Statistical Interpretation of Data—Part 6: Determination of Statistical Tolerance Intervals. International Organization for Standardization: Geneva, Switzerland, 2014.
59. Wu, C.-W.; Pearn, W.L.; Kotz, S. An Overview of Theory and Practice on Process Capability Indices for Quality Assurance. *Int. J. Prod. Econ.* **2009**, *117*, 338–359. [CrossRef]
60. Karaman, M.O.; Kulahci, M. Process Capability Indices: The Allure and the Perils of Summarizing Process Performance in a Single Index. *Qual. Eng.* **2025**, *37*, 513–522. [CrossRef]
61. *ISO 26262:2018*; Road Vehicles—Functional Safety (Parts 1–12). International Organization for Standardization: Geneva, Switzerland, 2018.
62. Fitzgerald, P.; Therkelsen, P.; Sheaffer, P.; Rao, P. Deeper and Persistent Energy Savings and Carbon Dioxide Reductions Achieved through ISO 50001 in the Manufacturing Sector. *Sustain. Energy Technol. Assess.* **2023**, *57*, 103280. [CrossRef]
63. Miera, K.; Botts, A.; Lemar, P.; Kamath, D.; Wenning, T. Unlocking Manufacturing Sustainability: Energy Efficiency Opportunities through the US Department of Energy's Better Plants Program Energy Treasure Hunts (2023–2024). *Sustainability* **2024**, *16*, 7918. [CrossRef]
64. Zhang, Z.; Li, Y.; Yoon, S.W.; Won, D. Stage-Based Neural Network for Reflow Profile Prediction and Reflow Recipe Optimization for Quality and Energy-Saving. *Int. J. Adv. Manuf. Technol.* **2025**, *137*, 1745–1757. [CrossRef]
65. Schulze, M.; Nehler, H.; Ottosson, M.; Thollander, P. Energy Management in Industry—A Systematic Review of Previous Findings and an Integrative Conceptual Framework. *J. Clean. Prod.* **2016**, *112*, 3692–3708. [CrossRef]
66. Cagno, E.; Accordini, D.; Thollander, P.; Andrei, M.; Hasan, A.S.M.M.; Pessina, S.; Trianni, A. Energy Management and Industry 4.0: Analysis of the Enabling Effects of Digitalization on the Implementation of Energy Management Practices. *Appl. Energy* **2025**, *390*, 125877. [CrossRef]
67. Duflou, J.R.; Sutherland, J.W.; Dornfeld, D.; Herrmann, C.; Jeswiet, J.; Kara, S.; Hauschild, M.; Kellens, K. Towards Energy and Resource Efficient Manufacturing: A Processes and Systems Approach. *CIRP Ann.* **2012**, *61*, 587–609. [CrossRef]

68. Psarommatis, F.; Sousa, J.; Mendonça, J.P.; Kiritsis, D. Zero-Defect Manufacturing the Approach for Higher Manufacturing Sustainability in the Era of Industry 4.0: A Position Paper. *Int. J. Prod. Res.* **2022**, *60*, 73–91. [CrossRef]
69. Powell, D.; Magnanini, M.C.; Colledani, M.; Myklebust, O. Advancing Zero Defect Manufacturing: A State-of-the-Art Perspective and Future Research Directions. *Comput. Ind.* **2022**, *136*, 103596. [CrossRef]
70. Gal, B.; Madreiter, T.; Scheder, N.; Liesinger, E.; Hold, P.; Schlund, S. Expanding the Boundaries of Zero Defect Manufacturing—A Systematic Literature Review. *Procedia CIRP* **2024**, *122*, 336–341. [CrossRef]
71. Psarommatis, F.; May, G. Optimization of Zero Defect Manufacturing Strategies: A Comparative Study on Simplified Modeling Approaches for Enhanced Efficiency and Accuracy. *Comput. Ind. Eng.* **2024**, *187*, 109783. [CrossRef]
72. Carvalho, T.P.; Soares, F.A.A.M.N.; Vita, R.; Francisco, R.d.P.; Basto, J.P.; Alcalá, S.G.S. A Systematic Literature Review of Machine Learning Methods Applied to Predictive Maintenance. *Comput. Ind. Eng.* **2019**, *137*, 106024. [CrossRef]
73. Serradilla, O.; Zugasti, E.; Rodriguez, J.; Zurutuza, U. Deep Learning Models for Predictive Maintenance: A Survey, Comparison, Challenges and Prospects. *Appl. Intell.* **2022**, *52*, 10934–10964. [CrossRef]
74. Li, W.; Li, T. Comparison of Deep Learning Models for Predictive Maintenance in Industrial Manufacturing Systems Using Sensor Data. *Sci. Rep.* **2025**, *15*, 23545. [CrossRef] [PubMed]

Disclaimer/Publisher's Note: The statements, opinions and data contained in all publications are solely those of the individual author(s) and contributor(s) and not of MDPI and/or the editor(s). MDPI and/or the editor(s) disclaim responsibility for any injury to people or property resulting from any ideas, methods, instructions or products referred to in the content.